ACS OMEGA

http://pubs.acs.org/journal/acsodf

Article

Proteomic Analysis Reveals Distinct Protein Corona Compositions of Citrate- and Riboflavin-Coated SPIONs

Wid Mekseriwattana, Tipparat Thiangtrongjit, Onrapak Reamtong, Patompon Wongtrakoongate, and Kanlaya Prapainop Katewongsa*

Cite This: *ACS Omega* 2022, 7, 37589–37599

Read Online

ACCESS | Metrics & More | Article Recommendations | Supporting Information

ABSTRACT: Superparamagnetic iron oxide nanoparticles (SPIONs) are recognized as one of the most beneficial tools for biomedicine, especially in theranostic applications. Even though SPIONs have excellent properties regarding their biocompatibility and unique magnetic properties, they lack stability in biological fluids. To stabilize and increase the specificity of the SPIONs to target desirable cells or tissues, several surface coatings have been introduced. These surface coatings can lead to different preferences of serum protein bindings, which ultimately determine their behaviors *in vitro* and *in vivo*. Thus, understanding the interaction of SPIONs with biological systems is important for their biocompatible design and clinical applications. In this study, using proteomic analyses, we analyzed the protein corona fingerprints on SPIONs with two different coatings, including citrate and riboflavin, that have been widely used as surface coatings and ligands for enhancing cellular uptake in breast cancer cells. Though both citrate-coated SPIONs (C-SPIONs) and riboflavin-coated SPIONs (Rf-SPIONs) showed similar sizes and zeta potentials, we found that Rf-SPIONs adsorbed more serum proteins than bare SPIONs (B-SPIONs) or C-SPIONs, which was likely due to the higher hydrophobicity of the riboflavin. The enriched proteins consisted mainly of immune-responsive and blood coagulation proteins with different fingerprint profiles. Cellular uptake studies in MCF-7 breast cancer cells comparing the activities of preformed and *in situ* coronas showed different uptake behaviors, suggesting the role of protein corona formation in promoting the interaction between the SPIONs and the cells. The results obtained here provide the essential information for further development of the potential strategy to reduce or stimulate immune response *in vivo* to increase therapeutic applications of both C-SPIONs and Rf-SPIONs.

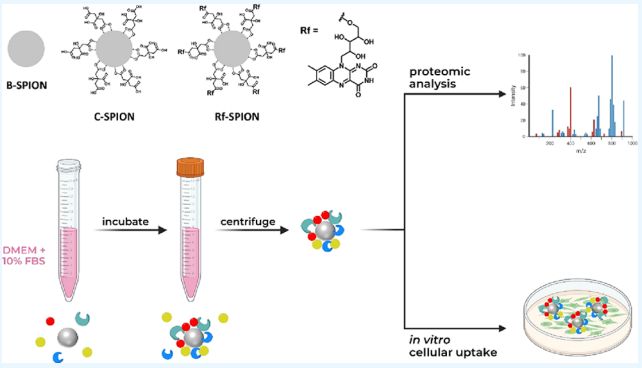

1. INTRODUCTION

In the past decades, superparamagnetic iron oxide nanoparticles (SPIONs) have been extensively studied and utilized as contrasting agents in magnetic resonance imaging (MRI) and for treatment in magnetic hyperthermia (MH) due to their excellent biocompatibility and magnetic properties. To improve their stability in biological fluids and increase their specificity to target sites, several surface coatings have been introduced.[1,2] Different surface coatings can lead to different preferences of protein binding on the surface of nanoparticles (NPs) called "protein corona", which ultimately determines its behavior *in vitro* and *in vivo*.[3] The most evident outcome is in the interaction of NPs with macrophages which directly affect their circulation time.[4,5] Furthermore, formation of protein coronas can alter the toxicity of the NPs toward mammalian cells in both positive[6,7] and negative ways.[8,9] Therefore, the study of protein corona compositions, even though not sufficient for full prediction, could provide us a brief context of how the NPs would interact with their biological environments, which is important for their safe design and efficient biomedical applications.

With the revelation of its importance, the study of corona compositions of different types of NPs became of interest. This was made possible through the development of shotgun proteomic techniques. A past study on poly(lactic-*co*-glycolic acid) (PLGA) NPs showed that the corona compositions changed in response to their surface chemistry but not to the particle sizes.[10] Similar studies were done for coronas of iron oxide nanoparticles by Sakulkhu *et al.*, and they found that size and surface charges of the SPIONs influenced both the corona compositions and their binding strength.[11] Further studies by the same group revealed that the surface chemistry of SPIONs

Received: July 14, 2022
Accepted: September 29, 2022
Published: October 12, 2022

https://doi.org/10.1021/acsomega.2c04440
ACS Omega 2022, 7, 37589–37599

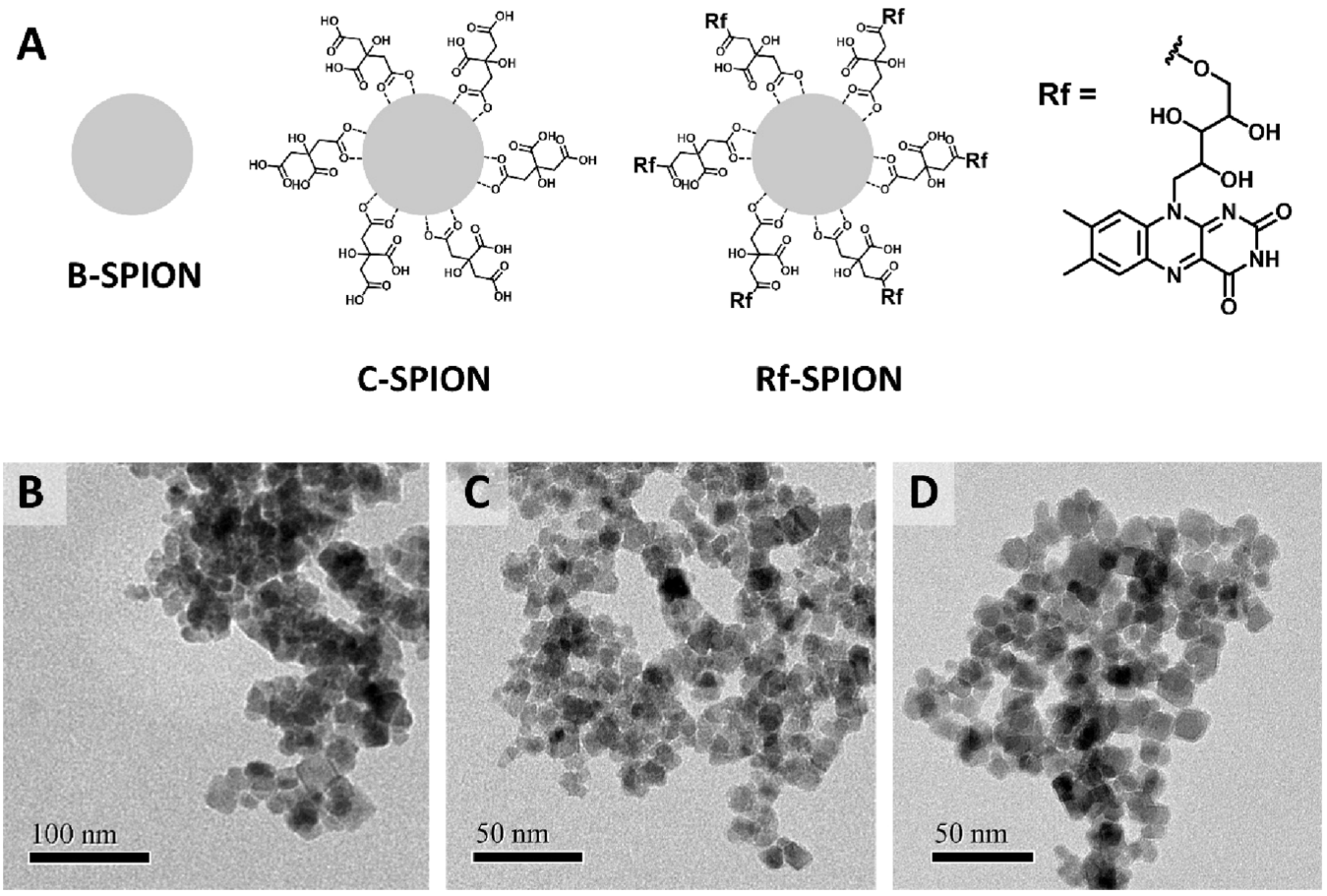

Figure 1. (A) Scheme representing the surface chemistry of B-, C-, and Rf-SPIONs. (B–D) TEM images of B-, C-, and Rf-SPIONs, respectively.

also plays a huge role in determining their interactions with serum proteins.[12]

To further address this aspect, here we study the composition of protein corona on the SPIONs in fetal bovine serum (FBS) for three types of particles, bare SPIONs (B-SPIONs), citrate-coated SPIONs (C-SPIONs), and riboflavin-coated SPIONs (Rf-SPIONs) through proteomic analyses. Citric acid is one of the most commonly used anionic surface stabilizers for SPIONs.[13] In addition, riboflavin (Rf) is also a promising ligand that has been increasingly used on several types of particles such as PLGA, dendrimer, or SPIONs due to its property of enhancing cellular uptake in several estrogen-related cancer cells.[14,15] It has been shown recently by our group that multicore SPIONs with both surface coatings have excellent properties as MRI contrast agents and MH agents.[2] The SPIONs, having a clustered morphology, exhibit exceptionally high T_2 values, which can be considered as one of the highest T_2 responses among the SPIONs synthesized from co-precipitation methods. Their MH responses were also considerably sufficient for tumor heating when excited with the alternating magnetic field under biological limits. Here, to compare their corona compositions, corona proteins were analyzed in terms of their physical properties and biological activities. A distinct corona binding pattern was found from the Rf-SPIONs and could be related to their enhanced cellular internalization in breast cancer cells.

2. EXPERIMENTAL SECTION

2.1. Materials. Ammonium bicarbonate (NH_4HCO_3), dithiothreitol (DTT), α-iodoacetamide, acetonitrile, formic acid, and trypsin were obtained from Sigma-Aldrich. Coomassie blue G-250 was purchased from Bio-Rad, CA, USA. MCF-7 (HTB22) cells were purchased from American Type Culture Collection (ATCC). All cell culture materials, including Dulbecco's modified Eagle's medium (DMEM), FBS (lot number: 42A0071K), penicillin/streptomycin solution (P/S), and trypsin–EDTA solution were obtained from Gibco, UK.

2.2. Synthesis of SPIONs. B-SPIONs were prepared according to the previously reported methods by a co-precipitation synthesis of $FeCl_2$ and $FeCl_3$ under basic conditions.[2] Coating of the SPIONs was further done either by using trisodium citrate dihydrate to yield C-SPIONs, or Rf conjugate[2] to yield Rf-SPIONs. The coating process involved mixing B-SPIONs (50 mg) and the ligand (50 mg) in Milli-Q water and heated at 90 °C under vigorous stirring for 90 min. The resulting SPIONs were washed and separated by magnetic decantation for C-SPIONs and by centrifugation at 10,000 rpm for Rf-SPIONs. The scheme and the TEM images of the bare and coated SPIONs are shown in Figure 1.

2.3. Protein Corona Formation. B-, C-, or Rf-SPIONs were dispersed in DMEM containing 10% of FBS to the final concentration of 0.2 mg mL^{-1} in a low-retention microtube. The tubes were placed upright and incubated for 1 h at 37 °C under constant shaking at 100 rpm. After incubation, the SPION coronas were isolated by centrifugation at 9500 g for

https://doi.org/10.1021/acsomega.2c04440
ACS Omega 2022, 7, 37589–37599

10 min and washed with PBS. The processes were repeated twice, and the coronas were stored at 4 °C for further analyses. Here on, the coronas will be referred to as corona@B-SPION, corona@C-SPION, and corona@Rf-SPION.

2.4. Hydrodynamic Diameter Measurement. The hydrodynamic diameter (D_H) of the coronas was measured by dynamic light scattering technique using a Zetasizer Ultra (Malvern Panalytical, UK). The samples were prepared by dispersing the isolated coronas in 1 mL of Milli-Q water or non-supplemented DMEM to the final concentration of 0.01 mg_{SPION} mL^{-1} immediately before the size determination.

2.5. Identification of Protein Corona by SDS-PAGE. The corona@SPION pellets were resuspended in Laemmli loading buffer (Sigma-Aldrich) and denatured by heating at 90 °C for 10 min. Each sample, containing 75 μg equivalent amount of SPIONs, was loaded onto 12% SDS-polyacrylamide gels. A constant electrical voltage of 120 V was applied to the gels until the front dye reached the bottom of the gels. The separated protein bands were visualized by staining with Coomassie blue G-250. The intensity of each lane was measured and reported as the relative intensity to the marker lane using Fiji software.[16]

2.6. In-Gel Digestion. Each gel lane was excised into 12 pieces and was destained separately in a solution of 50% acetonitrile in 25 mM NH_4HCO_3 overnight. After destaining, proteins were reduced using 4 mM DTT in 50 mM NH_4HCO_3 solution at 60 °C for 15 min. Proteins were then cysteine alkylated with 250 mM solution of α-iodoacetamide for 30 min in dark conditions. The reaction was quenched with 4 mM DTT in 50 mM NH_4HCO_3 for 5 min at room temperature. The gel pieces were dehydrated in acetonitrile and left for 1 h to dry. To digest the peptides, 10 μg mL^{-1} solution of proteomics-grade trypsin in 50 mM NH_4HCO_3 was added and left at room temperature for 15 min. Acetonitrile and 50 mM NH_4HCO_3 were added, and the gel pieces were incubated at 37 °C overnight. Finally, the fractions of supernatant containing the extracted peptides were collected and dried by a centrifugal evaporator (TOMY, Japan). Each sample was prepared in three independent replicates, and the samples were stored at −20 °C until further use.

2.7. Protein Identification by Mass Spectrometry. The peptides were resuspended in 0.1% formic acid and injected into UltiMate 3000 nano-liquid chromatography (nano-LC) systems (Dionex, Surrey, UK). Peptides were separated using a C18 column (Thermo Scientific, Waltham, MA) at a flow rate of 300 nL min^{-1}. Mobile phase A was 0.1% formic acid in water and mobile phase B was 80% acetonitrile in 0.1% formic acid. The elution was done by a 30 min gradient from 4% mobile phase B to 50% mobile phase A. The separated peptides were then infused to a micrOTOF-Q (Bruker Daltonics, Bremen, Germany). The mass spectrometry and tandem mass spectrometry covered the mass ranges of m/z 400−2000 and m/z 50−1500, respectively. The mass spectrometric data were processed and converted to MGF (Mascot Generic Format) using DataAnalysis software. The MGF files were searched against the UniProtKB/Swiss-Prot mammalian database [downloaded on February 2, 2019, containing 515203 reviewed sequences using Mascot Daemon software (version 2.3.02, Matrix Science, USA)].

2.8. Data Analysis. The protein quantities were reported as the exponentially modified protein abundance index (emPAI) value.[17] Keratins were discarded from the identified protein pools. The remaining proteins were screened by selection of bovine-associated proteins. Following the screening, the proteins which were identified in only one replicate were discarded. The remaining were then classified according to their biological functions based on gene ontology using UniProtKB (https://www.uniprot.org) as blood coagulation (BC) proteins, immune response (IR) proteins, lipoproteins (LP), regulation of insulin-like growth factor (IGF), oxygen transport (OT) proteins, and other serum components (OC). Other protein properties were also summarized and used for comparison, including the isoelectric point (pI) and weight-average molecular weight (M_w).

2.9. Cell Culture. MCF-7 breast cancer cells were cultured in DMEM supplemented with 10% FBS and 1% P/S. Cells were maintained at 37 °C with 5% CO_2 in a humidified incubator. Subculture was done at 80% confluency using 0.25% trypsin−EDTA, and the media were changed every 4 days.

2.10. *In Vitro* Cellular Uptake. Cells were seeded into a 6-well plate (2 mL, 2×10^5 cells mL^{-1}). After incubation for 24 h, the media were discarded and replaced with fresh serum-supplemented DMEM containing 100 μg mL^{-1} of the preformed corona@SPIONs. Another set of experiments were performed by treating the cells with SPIONs, freshly dispersed in media, to evaluate the cellular uptake of the coronas when they are formed *in situ*. After incubation (4, 12, and 24 h), the media were discarded, and the cells were washed once with PBS and trypsinized before fresh DMEM were added. Then, the cells were transferred to a microtube and collected by centrifugation (1924 g, 5 min). Collected cells were rinsed with ice-cold PBS, followed by fixation with 3.6% formaldehyde on ice. After fixation, cells were separated by centrifugation and redispersed in PBS. Flow cytometry was performed using Attune NxT (ThermoFisher Scientific, MA, USA) and BD Accuri C6 plus (BD, NJ, USA) flow cytometers, where a fixed number of 10,000 gated events were collected and analyzed. Gating was done by following the reported method,[18] and the cellular uptake levels were evaluated by measuring the mean side scattering signal (SSC-A) of each treatment condition and normalized by the signals of the control experiments.

3. RESULTS

3.1. Corona@SPION Formation. Protein coronas of the SPIONs were formed by incubating the NPs in FBS-supplemented cell culture media. Formation of the coronas was first observed by increasing the D_H of the SPIONs. The initial D_H of all the SPIONs, including B-, C-, and Rf-SPIONs, were approximately 100−150 nm. Following corona formation, the D_H increased to approximately 300 nm for B- and C-SPIONs, and up to 400 nm in case of the corona@Rf-SPION when dispersed in water or DMEM. Another evidence of corona formation was observed from the change of zeta potential as shown in B-SPIONs where the zeta potential shifted from a positive to a negative value upon formation of corona@B-SPION. The complete D_H of the SPIONs and the coronas are summarized in Table 1.

The coronas were then isolated and subjected to SDS-PAGE where the protein patterns were observed by Coomassie blue staining (Figure 2A). From the gel, distinct protein pattern and amount as indicated by different band intensities of each corona were observed. Overall, the major protein bands were observed in the regions of 55 to over 180 kDa, with the most intense band appearing at approximately 70 kDa. The intensity of each lane, which corresponds to the amount of the proteins,

https://doi.org/10.1021/acsomega.2c04440
ACS Omega 2022, 7, 37589−37599

Table 1. D_H and Zeta Potential of the SPIONs and Their Protein Corona−SPION Complexes in Different Dispersion Media

Sample	dispersion media	D_H (nm)	PdI	zeta potential (mV)
B-SPIONs	water	143 ± 2	0.2	22 ± 0.5
	DMEM	1347 ± 37	0.3	
C-SPIONs	water	122 ± 0.3	0.2	−34 ± 0.4
	DMEM	870 ± 21	0.3	
Rf-SPIONS	water	119 ± 1	0.2	−35 ± 1
	DMEM	805 ± 16	0.2	
corona@B-SPION	water	273 ± 3	0.2	−34 ± 1
	DMEM	236 ± 2	0.2	
corona@C-SPION	water	260 ± 1	0.2	−30 ± 0.3
	DMEM	353 ± 3	0.3	
corona@Rf-SPION	water	346 ± 2	0.4	−34 ± 0.3
	DMEM	412 ± 29	0.4	

was analyzed using Fiji software and presented in Figure 2B. Of the three samples, corona@Rf-SPION (lane 3) showed the highest lane intensity, followed by corona@C-SPION and corona@B-SPION, respectively (lanes 2 and 1).

3.2. Proteomic Analysis of the Coronas. Following SDS-PAGE, the gels were excised, and the corona proteins were digested into peptides. The peptides were subjected to LC−MS/MS and interpreted on their fragmentation data to identify the proteins in the coronas. Here, the coronas were prepared and analyzed in three biological replicates, and the proteins identified in at least two replicates were selected for further analysis (full lists of identified proteins are shown in Tables S1−S3).

From the analyses, approximately 40 different proteins were identified from the coronas of B- and C-SPIONs, while a higher number of over 50 proteins was found from the Rf-SPION corona. When grouped according to the type of coronas (Figure 3A), 22 proteins were found to be common between the three coronas. The corona@B-SPION and corona@Rf-SPION have 17 unique proteins, while the number was 2 for corona@C-SPION. Interestingly, C- and Rf-SPIONs share the highest number of 35 common proteins, compared to 25 proteins shared between B- and Rf-SPIONs and 24 proteins between B- and C-SPIONs.

The identified proteins from each corona were then categorized according to their physical properties (Figure 3B,C). The distribution of M_w of the corona proteins was similar between each sample. Almost 80% of proteins was found to have a M_w lower than 72 kDa. The distribution patterns of the pI of the corona proteins were also similar between groups, where around 60% of the identified proteins showed pI values between 4 and 7.

The proteins were further categorized into six groups according to their biological functions, as shown in Figure 3D: LP, IR proteins, OT proteins, proteins associated with the regulation of IGF, BC proteins , and the rest as OC. Again, the patterns of the biological functions were similar between the coronas of different SPIONs. When considering the proteins with specific functions (disregarding OC proteins), IR were found to be the major group of proteins in the coronas, especially in Rf-SPIONs. The second highest proteins found were in the group of BC, and followed by the minimal numbers of LP, OT, and IGF.

The affinity of each type of SPIONs toward different serum proteins was evaluated by comparing the emPAI values. The top 20 most abundant proteins in each corona are listed in Tables 2, 3, 4. Interesting proteins, including serum albumin, clusterin, complement factors, and apolipoproteins, were picked from the protein pool and their abundances were compared as shown in Figure 3E. Corona@B-SPION showed the least protein abundances among the three samples. The most abundant protein found was serum albumin, while the affinities with complement factors and apolipoproteins were minimal. In contrast, C- and Rf-SPIONs showed higher affinities toward all the proteins, except for apolipoprotein A-II which was not observed in Rf-SPION corona.

3.3. Cellular Uptake of the Corona-SPIONs in Breast Cancer Cells. Prior to cellular uptake experiments, the biocompatibility of the SPIONs with the cells was ensured by performing MTT cell viability assay and the results are shown in Figure S1. The impact of corona formation on cellular uptake was evaluated in MCF-7 breast cancer cells

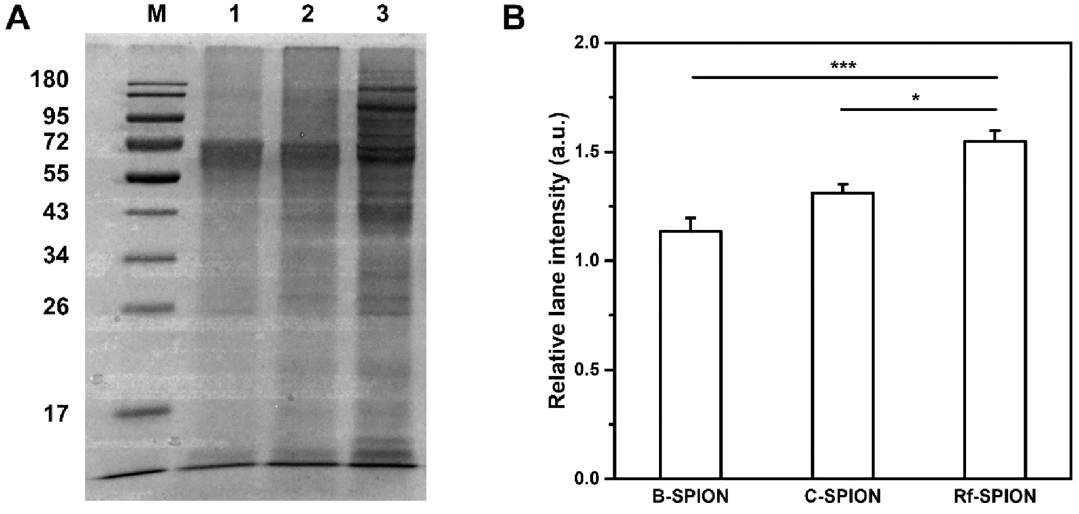

Figure 2. (A) SDS-PAGE results for protein coronas of B-, C-, and Rf-SPIONs (lanes 1, 2, and 3, respectively). Lane M represents the protein markers with M_w in kDa marked. (B) Overall intensities of each sample from the SDS-PAGE gel analyzed using Fiji software. Statistical significance was analyzed by one-way ANOVA with $p < 0.05$ (*) and $p < 0.001$ (***).

https://doi.org/10.1021/acsomega.2c04440
ACS Omega 2022, 7, 37589−37599

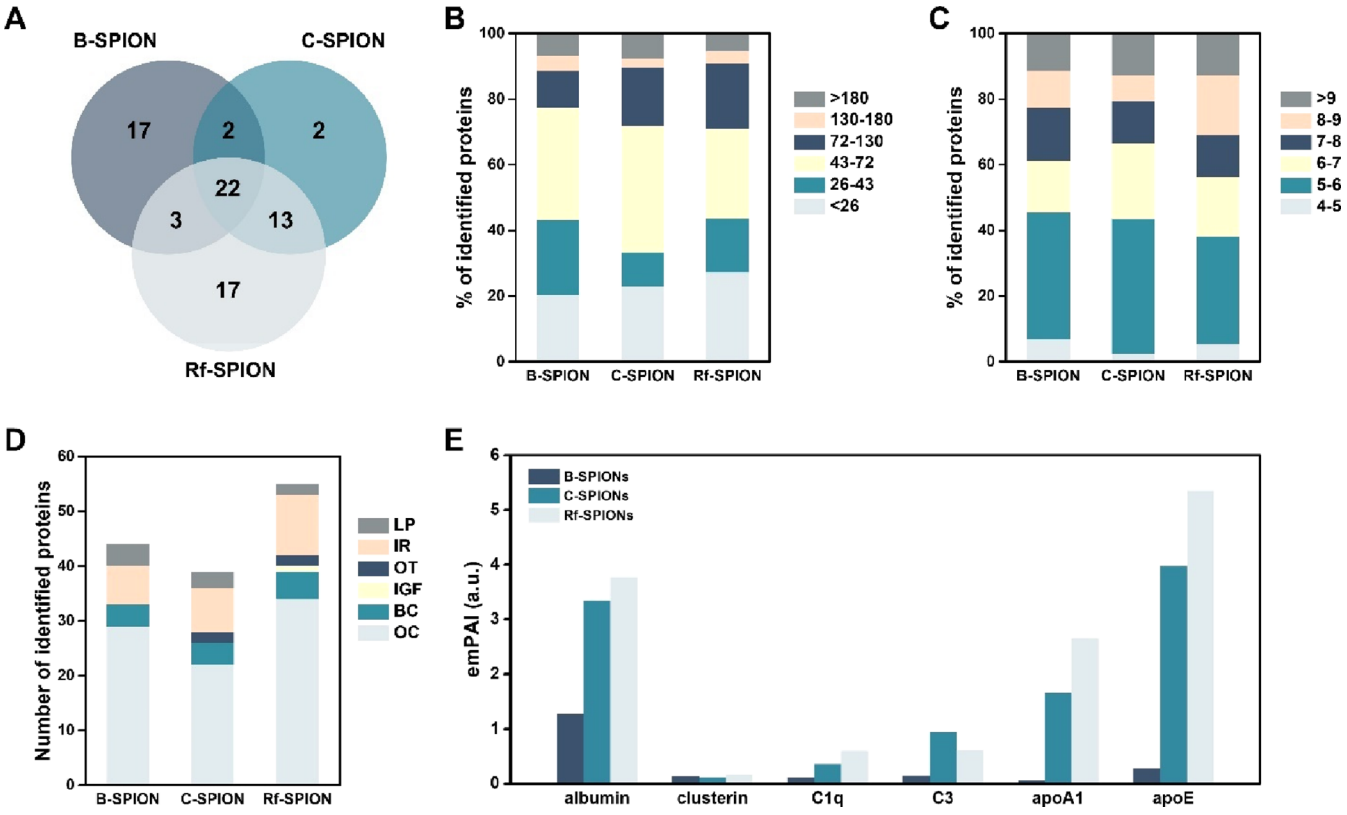

Figure 3. (A) Numbers of identified proteins in corona of each SPIONs. (B) Corona proteins categorized by their M_w (kDa). (C) Corona proteins categorized by their pI. (D) Corona proteins categorized by their biological functions (LP = lipoproteins, IR = immune-responsive, OT = oxygen transport, IGF = insulin-like growth factor, BC = blood coagulation, and OC = other serum components). (E) emPAI values of the proteins of interest.

Table 2. Top 20 Most Abundant Proteins Enriched in B-SPION Corona

protein accession	protein description	M_w (kDa)	emPAI
A1AT_BOVIN	α-1-antiproteinase	46	3.68
AMBP_BOVIN	protein AMBP	39	2.33
FETA_BOVIN	α-fetoprotein	69	2.21
ALBU_BOVIN	serum albumin	69	1.27
BPT2_BOVIN	spleen trypsin inhibitor I	11	0.77
ANT3_BOVIN	antithrombin-III	52	0.68
GELS_BOVIN	gelsolin	81	0.65
CO2A1_BOVIN	collagen α-1(II) chain (fragments)	71	0.65
CHRD1_BOVIN	cysteine and histidine-rich domain-containing protein 1	37	0.56
EZRI_BOVIN	ezrin	69	0.50
ACTH_BOVIN	actin, γ-enteric smooth muscle	42	0.40
CFAB_BOVIN	complement factor B	85	0.38
CASK_BOVIN	κ-casein	21	0.38
CP3AS_BOVIN	cytochrome P450 3A28	58	0.36
COF2_BOVIN	cofilin-2	19	0.36
DDX52_BOVIN	probable ATP-dependent RNA helicase DDX52	67	0.35
FA10_BOVIN	coagulation factor X	54	0.31
APOA2_BOVIN	apolipoprotein A-II	11	0.28
APOE_BOVIN	apolipoprotein E	36	0.27
CFAH_BOVIN	complement factor H	140	0.15

Table 3. Top 20 Most Abundant Proteins Enriched in C-SPION Corona

protein accession	protein description	M_w (kDa)	emPAI
HBBF_BOVIN	hemoglobin fetal subunit beta	16	19.15
HBA_BOVIN	hemoglobin subunit alpha	15	6.67
TETN_BOVIN	tetranectin	22	4.36
APOE_BOVIN	apolipoprotein E	36	3.97
ALBU_BOVIN	serum albumin	69	3.34
APOA2_BOVIN	apolipoprotein A-II	11	2.96
FETUA_BOVIN	α-2-HS-glycoprotein	38	2.41
APOA1_BOVIN	apolipoprotein A-I	30	1.66
CFAH_BOVIN	complement factor H	140	1.29
ANT3_BOVIN	antithrombin-III	52	0.97
CO3_BOVIN	complement C3	187	0.93
CO4_BOVIN	complement C4 (fragments)	102	0.56
A1AT_BOVIN	α-1-antiproteinase	46	0.48
LECT2_BOVIN	leukocyte cell-derived chemotaxin-2	16	0.46
TSP1_BOVIN	thrombospondin-1	129	0.45
TTHY_BOVIN	transthyretin	16	0.41
PEDF_BOVIN	pigment epithelium-derived factor	46	0.37
C1QA_BOVIN	complement C1q subcomponent subunit A	26	0.35
S10AC_BOVIN	protein S100-A12	11	0.32
COF1_BOVIN	cofilin-1	19	0.29

(Figure 4A). The uptake levels of all samples increased and saturated after 12 h incubation. Slight decreases were observed when the incubation time was prolonged to 24 h. Among the samples, corona@Rf-SPION has the highest cellular uptake activity, with the relative uptake reaching over 2.5 at 12 h. At

https://doi.org/10.1021/acsomega.2c04440
ACS Omega 2022, 7, 37589−37599

Table 4. Top 20 Most Abundant Proteins Enriched in Rf-SPION Corona

protein accession	protein description	M_w (kDa)	emPAI
HBBF_BOVIN	hemoglobin fetal subunit beta	16	34.32
HBA_BOVIN	hemoglobin subunit alpha	15	7.77
APOE_BOVIN	apolipoprotein E	36	5.35
ALBU_BOVIN	serum albumin	69	3.77
PPIA_BOVIN	peptidyl-prolyl cis−trans isomerase A	18	3.36
APOA1_BOVIN	apolipoprotein A-I	30	2.65
TETN_BOVIN	tetranectin	22	2.26
CO4_BOVIN	complement C4 (fragments)	102	1.63
CFAH_BOVIN	complement factor H	140	1.63
FETUA_BOVIN	α-2-HS-glycoprotein	38	1.32
BPT2_BOVIN	spleen trypsin inhibitor I	11	1.17
GELS_BOVIN	gelsolin	81	1.14
TTHY_BOVIN	transthyretin	16	0.78
RNAS4_BOVIN	ribonuclease 4	14	0.69
CO3_BOVIN	complement C3	187	0.61
KLKB1_BOVIN	plasma kallikrein	71	0.56
LECT2_BOVIN	leukocyte cell-derived chemotaxin-2	16	0.56
ANT3_BOVIN	antithrombin-III	52	0.54
TSP1_BOVIN	thrombospondin-1	129	0.52
AMBP_BOVIN	protein AMBP	39	0.46

this condition, the relative uptake of corona@C-SPION was lower at approximately 1.7 and that of the corona@B-SPION was the lowest at 1.3.

By forming the coronas *in situ*, the trends of the cellular uptake were slightly altered. At 4 h, the uptake levels of all the SPIONs were comparable with the relative uptake of 1.5 (Figure 4B). Further incubation resulted in the similar trend of cellular uptake as observed from the preformed coronas. The level of Rf-SPIONs was the highest, followed by C- and B-SPIONs, respectively. The uptake levels at 24 h remained in the same trend to that of at 12 h but with lower overall activity.

4. DISCUSSION

The SPIONs used in this study were synthesized through a co-precipitation method, yielding aqueous-stable NPs with a D_H of approximately 120 nm. The coating of both citrate and Rf ligands was confirmed through the shift of zeta potential from the positive value in B-SPIONs to the negative values in both C- and Rf-SPIONs, which is due to the presence of carboxylic functional groups in both cases.

Following the corona formation, D_H of all the SPIONs increased to over 200 nm. This indicates the formation of the corona on the surface of the SPIONs. However, the size differences were larger than the normal size of the coronas observed from a monolayer or two-layer coatings.[19] This large increase could possibly be due to two reasons. First is that the morphologies of the starting SPIONs were not individual particles (Figure 1B−D), as normally found in SPIONs synthesized by co-precipitation methods where the SPIONs tend to form agglomerates due to the rapid seeding and growth of the NPs.[20] Therefore, the corona layers were not formed individually, and the size measured here would be the size of the clusters of the SPIONs, interacting with the corona proteins. Another reason could be the aggregation formed during the centrifugation process to isolate the coronas.[21] In addition, formation of the coronas provides stability to the SPIONs when dispersed in cell culture medium. The D_H of the naked SPIONs were found to be close to 1 μm, indicating severe aggregation (Table 1). While the sizes of the coronas remained approximately between 200 and 400 nm in DMEM.

The patterns of the coronas observed from SDS-PAGE showed that the Rf-SPIONs tended to have higher affinities to the serum proteins when compared to the others. The most intense band observed in all samples appeared at approximately 70 kDa could be attributed to the serum albumin (M_w = 67 kDa), which is the most abundant protein found in FBS.[22] In addition to the intensities, corona@Rf-SPION also showed a higher number of protein bands. For example, the bands appearing between 72 and 180 kDa were not observed in the lanes of B- and C-SPIONs. These results indicated that coating the SPIONs with the Rf ligand tends to increase the interaction of the SPIONs with the serum proteins. These changes in the protein interaction have proven not to be due to

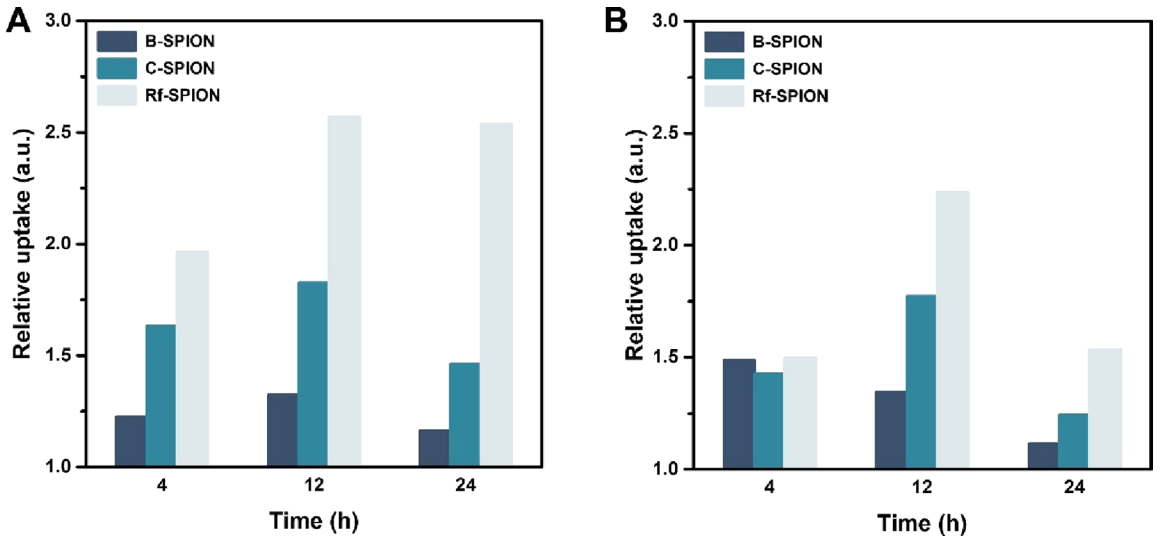

Figure 4. Cellular uptake levels of (A) preformed coronas and (B) coronas formed *in situ* in MCF-7 breast cancer cells.

https://doi.org/10.1021/acsomega.2c04440
ACS Omega 2022, 7, 37589−37599

the surface charges, since the protein bindings of B- and C-SPIONs were not different, despite the shifting of the surface charges from positive to negative (Figure 2A, lanes 1 and 2). In fact, it is likely due to the hydrophobicity of the surface. Even though Rf is known as a water-soluble vitamin, its aqueous solubility is very low when compared to that of citric acid (0.08 mg mL^{-1} for Rf[23] and 2 g mL^{-1} for citric acid[24] at room temperature). Therefore, the surface of the Rf-SPIONs is more hydrophobic when compared to the citrate coating in C-SPIONs and the hydroxyl-presenting B-SPIONs, which could be responsible for the significant differences in the protein binding property of the latter. This observation agrees with the previous research where NPs with a more hydrophobic surface tend to interact more with serum proteins.[25,26]

Next, the corona proteins were identified by injecting the digested peptides into an LC−MS/MS to obtain the mass spectra and the data were run against the mammalian SwissProt database. The proteins found in at least two out of three biological replicates were selected and the numbers of identified proteins are summarized in Figure 3A. Among the samples, corona@Rf-SPION showed the highest number of 55 bound proteins, which agrees with the SDS-PAGE results. In this number, 17 proteins were found to be unique. Interestingly, corona@Rf-SPION shared a high number of common proteins with corona@C-SPION with the number of 35 proteins. This is possibly due to the close proximity of the chemical structure of the ligands, as the Rf conjugate contains the citric acid moiety, providing a certain amount of similarities in their surface chemistry.

On the other hand, corona@B-SPION showed fewer common proteins with both corona@C-SPION and corona@Rf-SPION with the number of 24 common proteins each. This is expected as the surface chemistry and also the surface charge of B-SPIONs were different from the others. However, despite the difference in surface coatings, the three NPs shared 22 common corona proteins as summarized in Table 5. The majority of the proteins in this group tend to have high binding affinities with NPs, as they have been shown to bind to NPs in general, regardless of the core materials and surface chemistry. For example, α-1-antiproteinase, serum albumin, apolipoprotein A-I, coagulation factor V, and gelsolin were reported in the coronas of PLGA NPs.[10]

In the particular case of SPIONs, Sakulkhu *et al.* showed that this group of proteins is found in coronas of SPIONs with different surface chemistry and charges.[12] They also found that surface charges played a more dominant role in NP−protein interaction in SPIONs with polymeric coatings, which agrees with our hypothesis that here the coronas were affected more by the chemistry and hydrophobicity of the SPION surfaces. Their later work also showed that *ex situ* analysis of SPION coronas formed in rat models also have these groups of proteins as major components,[27] suggesting that the proteins such as albumin and apolipoproteins also interact strongly with SPIONs in more complex biological systems.

Recently, Portella *et al.* also found that SPIONs with different coatings share a large number of corona proteins.[28] They observed that most of these common proteins show affinity with divalent metals, suggesting that the incompletion of surface coatings allow the attachment of these proteins to the Fe atoms on the SPION surfaces. This resulted in the similar corona compositions between different types of SPION. The divalent metal-binding property agrees well with our results as the common proteins such as α-1-antiproteinase, albumin, gelsolin, and coagulation factor V all share this property.

Table 5. Common Proteins Found in corona@B-SPION, corona@C-SPION, and corona@Rf-SPION

protein accession	protein description
A1AT_BOVIN	α-1-antiproteinase
ALBU_BOVIN	serum albumin
AMBP_BOVIN	protein AMBP
ANT3_BOVIN	antithrombin-III
APOA1_BOVIN	apolipoprotein A-I
APOE_BOVIN	apolipoprotein E
C1QA_BOVIN	complement C1q subcomponent subunit A
CAP1_BOVIN	adenylyl cyclase-associated protein 1
CFAB_BOVIN	complement factor B
CFAH_BOVIN	complement factor H
CLUS_BOVIN	clusterin
CO1A2_BOVIN	collagen α-2(I) chain
CO3_BOVIN	complement C3
CO4_BOVIN	complement C4 (fragments)
CO7_BOVIN	complement component C7
CO9_BOVIN	complement component C9
COF1_BOVIN	cofilin-1
FA5_BOVIN	coagulation factor V
FETA_BOVIN	α-fetoprotein
FETUA_BOVIN	α-2-HS-glycoprotein
FINC_BOVIN	fibronectin
GELS_BOVIN	gelsolin

By categorizing the corona components according to their M_w and pI, the protein patterns appeared to be similar between each type of SPIONs (Figure 3B,C). Since the coronas were formed in cell culture media with pH of 7.6, the proteins with pI values of higher than 7.6 should have positive net charges and interact more with the C- and Rf-SPIONs, which possess negative surface charges, due to electrostatic interaction. In fact, the distribution patterns of pI appeared to be similar in all samples with almost 80% of the bound proteins having pI values between 4 and 8. These results support our hypothesis that the protein interaction here was not highly influenced from the surface charges of the SPIONs but rather by other factors such as hydrophobicity.

Further categorization of the proteins by their biological functions showed that the most abundant proteins found in all samples were IR proteins, followed by BC proteins. The first group consists mainly of complement proteins, which could be regarded as opsonins with the properties of activating clearance of the NPs by macrophages following their binding with the NPs.[29] For the interaction of the SPIONs with BC proteins, these could result in either a positive or a negative result, as previously reported with polystyrene NPs which can either increase or decrease the generation of thrombin in plasma with different surface functionalization.[30] Even though the effects of binding of NPs with BC proteins are not clear, hemostasis is a delicate balance, and a slight shift could lead to serious pathological processes.[31] Therefore, it is best to reduce the interaction of NPs with these groups of proteins, both IR and BC. Several strategies have been established in order to reduce these NP−protein interactions, including grafting of poly(ethylene glycol)[10] or preformation of protein corona with specific proteins.[32]

Despite the presence of IR and BC proteins, dysopsonins such as serum albumin were also found in the coronas of all

https://doi.org/10.1021/acsomega.2c04440
ACS Omega 2022, 7, 37589−37599

samples. Albumin, as one of the most abundant proteins in serum tends to have high affinity with NPs and has shown to be useful in stabilizing the NPs and prolong their blood circulation time *in vivo*.[33,34] Clusterin was another type of protein found in all coronas. The protein was also reported to have dysopsonic properties, giving stealth effects to the NPs against phagocytosis.[35,36] Therefore, the presence of the albumin and clusterin could counter the activities from the IR and BC proteins mentioned above.

Apolipoprotein is another interesting group of proteins. High-density lipoproteins (HDLs) such as apolipoprotein A-I and apolipoprotein E have been reported to have opsonin-like properties.[37] Despite that fact, the proteins also proved to be enhancing the abilities of NPs to cross the blood−brain barrier through interactions with brain endothelial cells.[38,39] Therefore, enrichment of these lipoproteins could not only affect the circulation time of the SPIONs but also be beneficial when targeting the NPs to brain tissues.

By comparing the abundance of each discussed protein between each type of coronas (Figure 3E), B-SPIONs have the least affinity with the proteins, followed by the C- and Rf-SPIONs, respectively. This is in good agreement with the prior results observed from SDS-PAGE where the lane intensities followed the same trend (Figure 2). Although the physical properties and number of types of the proteins found on each SPION were not much different (Figure 3A−D), the higher abundance of each protein suggested the effects of the coating materials such as citric acid and the Rf conjugate increasing the interaction of the SPIONs to the serum proteins. This increase in protein corona abundances could have a high influence on the NP behaviors when they are introduced *in vivo*, especially in terms of biodistribution and circulation time. This requires further investigation since, as discussed above that proteins such as albumin could help prolong the circulation time, while the high abundance of HDLs such as apolipoprotein A-I and apolipoprotein E could promote clearance through their opsonin-like properties.

Lastly, the uptake of the coronas in MCF-7 breast cancer cells was investigated. The results were compared between the uptake of preformed coronas and *in situ* coronas. By both treatments, corona@Rf-SPION showed the highest uptake activity, followed by corona@C-SPION and corona@B-SPION at almost every incubation time. The only difference was observed at the incubation time of 4 h, where by treating *in situ*, the uptake levels of all SPIONs were comparable, as opposed to the trend shown in preformed coronas. These different uptake patterns could be due to the delay in corona formation when the SPIONs were added *in situ* compared to the already formed coronas which were taken up faster. Therefore, this suggests the importance of corona proteins in facilitating the uptake of the SPIONs into the cells in a distinct manner between each type of SPION.

For other incubation times, Rf-SPIONs showed the highest uptake activity, regardless of the corona formation process. This agrees with the results that were reported earlier, where the Rf ligand significantly enhanced the internalization of the SPIONs in the breast cancer cell line.[2] The process was hypothesized to be facilitated by the interaction of the NPs with riboflavin carrier protein (RCP) or riboflavin transporters (RFVTs) overexpressed in breast cancer tissues.[40−42] Here, the results also showed that once the Rf-SPIONs interact with serum proteins, neither preformation nor *in situ* formation of the protein corona of Rf-SPIONs did affect the uptake efficiency of the particles. This is an interesting result as several works showed that formation of protein coronas could hinder the targeting efficiencies of NPs due to the coverage of the ligands, for example, in the transferrin-functionalized silica NPs.[43]

When comparing the uptake of each SPIONs (Figure 4A) with the protein abundance results (Figure 2B), the two factors tend to be correlated. The cellular uptake activity was found to be the highest in Rf-SPIONs, followed by C- and B-SPIONs, respectively, whose protein corona amounts followed the same trend. The breakdown of the interesting proteins showed a similar trend of abundance in each type of coronas (Figure 3E). As the most abundant protein in the serum, we investigated the effects of albumin on the cellular uptake of the SPIONs. The results, shown in Figure S2, indicate no observable effects from the albumin coronas in the uptake of the SPIONs in the breast cancer cells. These results are consistent with prior studies where albumin is reported to affect cellular uptake in negative ways as it has the property of reducing the interaction of the NPs with the surroundings such as other proteins or cell membranes.[44,45] Although not affecting directly, it is possible that albumin acts by reducing the non-specific interaction of the NPs with the cells, thereby allowing the Rf ligand to promote the interaction with the cells and resulting in the enhanced uptake of the Rf-SPIONs.

Other proteins that are possible to involve with the uptake of the NPs are apolipoproteins, including apolipoprotein A-I and apolipoprotein E. The proteins were reported to enhance the uptake of NPs into brain tissues due to their specific interaction with the receptors overexpressed in the blood−brain barrier.[37,46] However, the effects were not demonstrated in breast cancer cells beforehand.

Here, two hypotheses are suggested. One is that the coverage of the coronas did not affect the activities of the Rf ligand in promoting the cellular uptake activities. Another possible explanation is that there are distinct key components in the protein coronas of the Rf-SPIONs which help in increasing the uptake efficiency of the NPs into the cells. This requires further systemic analyses on the development of the coronas *in vitro* which could give more information on the proteins involved in the cell internalization processes.[47]

5. CONCLUSIONS

In this study, we characterized the protein corona components of our recently reported Rf-coated SPIONs in comparison with the bare and citrate-coated SPIONs. The results showed that the Rf ligand significantly promoted the interaction of the SPIONs with the serum proteins, as their corona components were distinct in terms of number of proteins found and overall protein amount. The effect was believed to be through the changes of the hydrophobicity of the SPION surface rather than the surface charge effects, as the physical properties including pI of the bound proteins were indifferent among the groups. Proteomic studies revealed high abundance of interesting proteins in the Rf-SPIONs, including serum albumin and apolipoproteins, which could render beneficial effects on the biodistribution of the SPIONs. However, the most abundant proteins in the coronas belong to the groups of IR proteins and BC factors. These results suggested that further development of the SPIONs is needed in order to reduce the unwanted protein binding prior to testing *in vivo*. Comparison of the cellular uptake between the preformed and *in situ* coronas in MCF-7 breast cancer cells showed the

https://doi.org/10.1021/acsomega.2c04440
ACS Omega 2022, 7, 37589−37599

difference in short-term incubation, which suggested the importance of protein coronas in promoting the high cellular uptake of C- and Rf-SPIONs. At prolonged incubation, both kinds of corona formation showed a similar uptake pattern where the highest activity was observed from Rf-SPIONs, followed by C- and B-SPIONs, respectively. The results highlighted the properties of the Rf ligand in promoting the cellular uptake of SPIONs in the breast cancer cells as reported earlier.[2] With no reduction of uptake levels in both cellular uptake processes, our hypotheses are that the corona proteins do not affect the activity of the Rf ligand in enhancing the cellular internalization or that there are key components in the corona influencing the uptake mechanism of the NPs. This would require further investigations in order to test the hypotheses.

■ ASSOCIATED CONTENT

Supporting Information

The Supporting Information is available free of charge at https://pubs.acs.org/doi/10.1021/acsomega.2c04440.

Protein corona components of corona @B-SPION, @C-SPION, and @Rf-SPION (PDF)

■ AUTHOR INFORMATION

Corresponding Author

Kanlaya Prapainop Katewongsa − *School of Materials Science and Innovation, Faculty of Science and Department of Biochemistry, Faculty of Science, Mahidol University, Bangkok 10400, Thailand;* orcid.org/0000-0001-6417-4921; Email: kanlaya.pra@mahidol.edu

Authors

Wid Mekseriwattana − *School of Materials Science and Innovation, Faculty of Science, Mahidol University, Bangkok 10400, Thailand*

Tipparat Thiangtrongjit − *Department of Molecular Tropical Medicine and Genetics, Faculty of Tropical Medicine, Mahidol University, Bangkok 10400, Thailand*

Onrapak Reamtong − *Department of Molecular Tropical Medicine and Genetics, Faculty of Tropical Medicine, Mahidol University, Bangkok 10400, Thailand*

Patompon Wongtrakoongate − *Department of Biochemistry, Faculty of Science and Center for Neuroscience, Faculty of Science, Mahidol University, Bangkok 10400, Thailand*

Complete contact information is available at: https://pubs.acs.org/10.1021/acsomega.2c04440

Notes

The authors declare no competing financial interest.

■ ACKNOWLEDGMENTS

This project was supported by Mahidol University under the New Discovery and Frontier Research grant (NDFR 08/2563 and NDFR 19/2564). This project was funded by the National Research Council of Thailand (NRCT) and Mahidol University: N42A650357. Partial support was also provided by the CIF and CNI grant, Faculty of Science, Mahidol University. W.M. was supported by the Science Achievement Scholarship of Thailand. P.W. was supported by Program Management Unit for Human Resources and Institutional Development, Research and Innovation (PMU-B; B05F640145). The authors thank Prof. Dr. Chutima Kuhakarn for support of the facilities for the synthesis of the Rf-citrate ligand.

■ REFERENCES

(1) Mekseriwattana, W.; Srisuk, S.; Kriangsaksri, R.; Niamsiri, N.; Prapainop, K. The impact of serum proteins and surface chemistry on magnetic nanoparticle colloidal stability and cellular uptake in breast cancer cells. *AAPS PharmSciTech* **2019**, *20*, 55.

(2) Mekseriwattana, W.; Guardia, P.; Herrero, B. T.; de la Fuente, J. M.; Kuhakarn, C.; Roig, A.; Katewongsa, K. P. Riboflavin−citrate conjugate multicore SPIONs with enhanced magnetic responses and cellular uptake in breast cancer cells. *Nanoscale Adv.* **2022**, *4*, 1988−1998.

(3) Lundqvist, M.; Stigler, J.; Elia, G.; Lynch, I.; Cedervall, T.; Dawson, K. A. Nanoparticle size and surface properties determine the protein corona with possible implications for biological impacts. *Proc. Natl. Acad. Sci. U.S.A.* **2008**, *105*, 14265−14270.

(4) Vogt, C.; Pernemalm, M.; Kohonen, P.; Laurent, S.; Hultenby, K.; Vahter, M.; Lehtiö, J.; Toprak, M. S.; Fadeel, B. Proteomics Analysis Reveals Distinct Corona Composition on Magnetic Nanoparticles with Different Surface Coatings: Implications for Interactions with Primary Human Macrophages. *PLoS One* **2015**, *10*, No. e0129008.

(5) Walkey, C. D.; Olsen, J. B.; Guo, H.; Emili, A.; Chan, W. C. Nanoparticle size and surface chemistry determine serum protein adsorption and macrophage uptake. *J. Am. Chem. Soc.* **2012**, *134*, 2139−2147.

(6) Wang, L.; Li, J.; Pan, J.; Jiang, X.; Ji, Y.; Li, Y.; Qu, Y.; Zhao, Y.; Wu, X.; Chen, C. Revealing the binding structure of the protein corona on gold nanorods using synchrotron radiation-based techniques: understanding the reduced damage in cell membranes. *J. Am. Chem. Soc.* **2013**, *135*, 17359−17368.

(7) Ortega, M. T.; Riviere, J. E.; Choi, K.; Monteiro-Riviere, N. A. Biocorona formation on gold nanoparticles modulates human proximal tubule kidney cell uptake, cytotoxicity and gene expression. *Toxicol. Vitro* **2017**, *42*, 150−160.

(8) Barbalinardo, M.; Caicci, F.; Cavallini, M.; Gentili, D. Protein Corona Mediated Uptake and Cytotoxicity of Silver Nanoparticles in Mouse Embryonic Fibroblast. *Small* **2018**, *14*, No. e1801219.

(9) Yoshida, T.; Yoshioka, Y.; Morishita, Y.; Aoyama, M.; Tochigi, S.; Hirai, T.; Tanaka, K.; Nagano, K.; Kamada, H.; Tsunoda, S.; Nabeshi, H.; Yoshikawa, T.; Higashisaka, K.; Tsutsumi, Y. Protein corona changes mediated by surface modification of amorphous silica nanoparticles suppress acute toxicity and activation of intrinsic coagulation cascade in mice. *Nanotechnology* **2015**, *26*, 245101.

(10) Partikel, K.; Korte, R.; Stein, N. C.; Mulac, D.; Herrmann, F. C.; Humpf, H. U.; Langer, K. Effect of nanoparticle size and PEGylation on the protein corona of PLGA nanoparticles. *Eur. J. Pharm. Biopharm.* **2019**, *141*, 70−80.

(11) Sakulkhu, U.; Mahmoudi, M.; Maurizi, L.; Salaklang, J.; Hofmann, H. Protein corona composition of superparamagnetic iron oxide nanoparticles with various physico-chemical properties and coatings. *Sci. Rep.* **2014**, *4*, 5020.

(12) Sakulkhu, U.; Mahmoudi, M.; Maurizi, L.; Coullerez, G.; Hofmann-Amtenbrink, M.; Vries, M.; Motazacker, M.; Rezaee, F.; Hofmann, H. Significance of surface charge and shell material of superparamagnetic iron oxide nanoparticle (SPION) based core/shell nanoparticles on the composition of the protein corona. *Biomater. Sci.* **2015**, *3*, 265−278.

(13) Li, L.; Mak, K. Y.; Leung, C. W.; Chan, K. Y.; Chan, W. K.; Zhong, W.; Pong, P. W. T. Effect of synthesis conditions on the properties of citric-acid coated iron oxide nanoparticles. *Microelectron. Eng.* **2013**, *110*, 329−334.

(14) Mekseriwattana, W.; Phungsom, A.; Sawasdee, K.; Wongwienkham, P.; Kuhakarn, C.; Chaiyen, P.; Katewongsa, K. P. Dual functions of riboflavin-functionalized poly(lactic-co-glycolic acid) nanoparticles for enhanced drug delivery efficiency and photodynamic therapy in triple-negative breast cancer cells. *Photochem. Photobiol.* **2021**, *97*, 1548−1557.

(15) Ribes, J.; Beztsinna, N.; Bailly, R.; Castano, S.; Rascol, E.; Taib-Maamar, N.; Badarau, E.; Bestel, I. Flavin-conjugated nanobombs: key structural requirements governing their self-assemblies' morphologies. *Bioconjugate Chem.* **2021**, *32*, 553−562.
(16) Schindelin, J.; Arganda-Carreras, I.; Frise, E.; Kaynig, V.; Longair, M.; Pietzsch, T.; Preibisch, S.; Rueden, C.; Saalfeld, S.; Schmid, B.; Tinevez, J. Y.; White, D. J.; Hartenstein, V.; Eliceiri, K.; Tomancak, P.; Cardona, A. Fiji: an open-source platform for biological-image analysis. *Nat. Methods* **2012**, *9*, 676−682.
(17) Ishihama, Y.; Oda, Y.; Tabata, T.; Sato, T.; Nagasu, T.; Rappsilber, J.; Mann, M. Exponentially modified protein abundance index (emPAI) for estimation of absolute protein amount in proteomics by the number of sequenced peptides per protein. *Mol. Cell. Proteomics* **2005**, *4*, 1265−1272.
(18) Youhannayee, M.; Nakhaei-Rad, S.; Haghighi, F.; Klauke, K.; Janiak, C.; Ahmadian, M. R.; Rabenalt, R.; Albers, P.; Getzlaff, M. Physical characterization and uptake of iron oxide nanoparticles of different prostate cancer cells. *J. Magn. Magn. Mater.* **2019**, *473*, 205−214.
(19) Moya, C.; Escudero, R.; Malaspina, D. C.; de la Mata, M.; Hernández-Saz, J.; Faraudo, J.; Roig, A. Insights into preformed human serum albumin corona on iron oxide nanoparticles: structure, effect of particle size, impact on MRI efficiency, and metabolization. *ACS Appl. Bio Mater.* **2019**, *2*, 3084−3094.
(20) LaGrow, A. P.; Besenhard, M. O.; Hodzic, A.; Sergides, A.; Bogart, L. K.; Gavriilidis, A.; Thanh, N. T. K. Unravelling the growth mechanism of the co-precipitation of iron oxide nanoparticles with the aid of synchrotron X-Ray diffraction in solution. *Nanoscale* **2019**, *11*, 6620−6628.
(21) Vauthier, C.; Cabane, B.; Labarre, D. How to concentrate nanoparticles and avoid aggregation? *Eur. J. Pharm. Biopharm.* **2008**, *69*, 466−475.
(22) Zheng, X.; Baker, H.; Hancock, W. S.; Fawaz, F.; McCaman, M.; Pungor, E., Jr. Proteomic analysis for the assessment of different lots of fetal bovine serum as a raw material for cell culture. Part IV. Application of proteomics to the manufacture of biological drugs. *Biotechnol. Prog.* **2006**, *22*, 1294−1300.
(23) Morrison, P. W.; Connon, C. J.; Khutoryanskiy, V. V. Cyclodextrin-mediated enhancement of riboflavin solubility and corneal permeability. *Mol. Pharm.* **2013**, *10*, 756−762.
(24) Oliveira, M. L. N.; Malagoni, R. A.; Franco, M. R. Solubility of citric acid in water, ethanol, n-propanol and in mixtures of ethanol +water. *Fluid Phase Equilib.* **2013**, *352*, 110−113.
(25) Cedervall, T.; Lynch, I.; Lindman, S.; Berggård, T.; Thulin, E.; Nilsson, H.; Dawson, K. A.; Linse, S. Understanding the nanoparticle-protein corona using methods to quantify exchange rates and affinities of proteins for nanoparticles. *Proc. Natl. Acad. Sci. U.S.A.* **2007**, *104*, 2050−2055.
(26) Lindman, S.; Lynch, I.; Thulin, E.; Nilsson, H.; Dawson, K. A.; Linse, S. Systematic investigation of the thermodynamics of HSA adsorption to N-iso-propylacrylamide/N-tert-butylacrylamide copolymer nanoparticles. Effects of particle size and hydrophobicity. *Nano Lett.* **2007**, *7*, 914−920.
(27) Sakulkhu, U.; Maurizi, L.; Mahmoudi, M.; Motazacker, M.; Vries, M.; Gramoun, A.; Ollivier Beuzelin, M. G.; Vallée, J. P.; Rezaee, F.; Hofmann, H. *Ex situ* evaluation of the composition of protein corona of intravenously injected superparamagnetic nanoparticles in rats. *Nanoscale* **2014**, *6*, 11439−11450.
(28) Portilla, Y.; Mellid, S.; Paradela, A.; Ramos-Fernández, A.; Daviu, N.; Sanz-Ortega, L.; Pérez-Yagüe, S.; Morales, M. P.; Barber, D. F. Iron oxide nanoparticle coatings dictate cell outcomes despite the influence of protein coronas. *ACS Appl. Mater. Interfaces* **2021**, *13*, 7924−7944.
(29) Papini, E.; Tavano, R.; Mancin, F. Opsonins and dysopsonins of nanoparticles: facts, concepts, and methodological guidelines. *Front. Immunol.* **2020**, *11*, 567365.
(30) Oslakovic, C.; Cedervall, T.; Linse, S.; Dahlbäck, B. Polystyrene nanoparticles affecting blood coagulation. *Nanomedicine* **2012**, *8*, 981−986.
(31) Ilinskaya, A. N.; Dobrovolskaia, M. A. Nanoparticles and the blood coagulation system. In *Handbook of Immunological Properties of Engineered Nanomaterials*; World Scientific Publishing Company, 2016; pp 261−302.
(32) Oh, J. Y.; Kim, H. S.; Palanikumar, L.; Go, E. M.; Jana, B.; Park, S. A.; Kim, H. Y.; Kim, K.; Seo, J. K.; Kwak, S. K.; Kim, C.; Kang, S.; Ryu, J. H. Cloaking nanoparticles with protein corona shield for targeted drug delivery. *Nat. Commun.* **2018**, *9*, 4548.
(33) Xia, B.; Zhang, W.; Shi, J.; Xiao, S. J. Engineered stealth porous silicon nanoparticles via surface encapsulation of bovine serum albumin for prolonging blood circulation in vivo. *ACS Appl. Mater. Interfaces* **2013**, *5*, 11718−11724.
(34) Peng, Q.; Zhang, S.; Yang, Q.; Zhang, T.; Wei, X. Q.; Jiang, L.; Zhang, C. L.; Chen, Q. M.; Zhang, Z. R.; Lin, Y. F. Preformed albumin corona, a protective coating for nanoparticles based drug delivery system. *Biomaterials* **2013**, *34*, 8521−8530.
(35) Aoyama, M.; Hata, K.; Higashisaka, K.; Nagano, K.; Yoshioka, Y.; Tsutsumi, Y. Clusterin in the protein corona plays a key role in the stealth effect of nanoparticles against phagocytes. *Biochem. Biophys. Res. Commun.* **2016**, *480*, 690−695.
(36) Schöttler, S.; Becker, G.; Winzen, S.; Steinbach, T.; Mohr, K.; Landfester, K.; Mailänder, V.; Wurm, F. R. Protein adsorption is required for stealth effect of poly(ethylene glycol)- and poly-(phosphoester)-coated nanocarriers. *Nat. Nanotechnol.* **2016**, *11*, 372−377.
(37) Fedeli, C.; Segat, D.; Tavano, R.; De Franceschi, G.; de Laureto, P. P.; Lubian, E.; Selvestrel, F.; Mancin, F.; Papini, E. Variations of the corona HDL:albumin ratio determine distinct effects of amorphous SiO_2 nanoparticles on monocytes and macrophages in serum. *Nanomedicine* **2014**, *9*, 2481−2497.
(38) Dal Magro, R.; Albertini, B.; Beretta, S.; Rigolio, R.; Donzelli, E.; Chiorazzi, A.; Ricci, M.; Blasi, P.; Sancini, G. Artificial apolipoprotein corona enables nanoparticle brain targeting. *Nanomedicine* **2018**, *14*, 429−438.
(39) Xiao, W.; Wang, Y.; Zhang, H.; Liu, Y.; Xie, R.; He, X.; Zhou, Y.; Liang, L.; Gao, H. The protein corona hampers the transcytosis of transferrin-modified nanoparticles through blood-brain barrier and attenuates their targeting ability to brain tumor. *Biomaterials* **2021**, *274*, 120888.
(40) Rao, P. N.; Levine, E.; Myers, M. O.; Prakash, V.; Watson, J.; Stolier, A.; Kopicko, J. J.; Kissinger, P.; Raj, S. G.; Raj, M. H. Elevation of serum riboflavin carrier protein in breast cancer. *Cancer Epidemiol. Biomarkers Prev.* **1999**, *8*, 985−990.
(41) Karande, A. A.; Sridhar, L.; Gopinath, K. S.; Adiga, P. R. Riboflavin carrier protein: a serum and tissue marker for breast carcinoma. *Int. J. Cancer* **2001**, *95*, 277−281.
(42) Bartmann, L.; Schumacher, D.; von Stillfried, S.; Sternkopf, M.; Alampour-Rajabi, S.; van Zandvoort, M.; Kiessling, F.; Wu, Z. Evaluation of riboflavin transporters as targets for drug delivery and theranostics. *Front. Pharmacol.* **2019**, *10*, 79.
(43) Salvati, A.; Pitek, A. S.; Monopoli, M. P.; Prapainop, K.; Bombelli, F. B.; Hristov, D. R.; Kelly, P. M.; Åberg, C.; Mahon, E.; Dawson, K. A. Transferrin-functionalized nanoparticles lose their targeting capabilities when a biomolecule corona adsorbs on the surface. *Nat. Nanotechnol.* **2013**, *8*, 137−143.
(44) Allouni, Z. E.; Gjerdet, N. R.; Cimpan, M. R.; Høl, P. J. The effect of blood protein adsorption on cellular uptake of anatase TiO_2 nanoparticles. *Int. J. Nanomed.* **2015**, *10*, 687−695.
(45) Li, T.; Wang, Y.; Wang, M.; Zheng, L.; Dai, W.; Jiao, C.; Song, Z.; Ma, Y.; Ding, Y.; Zhang, Z.; Yang, F.; He, X. Impact of albumin pre-coating on gold nanoparticles uptake at single-cell level. *Nanomaterials* **2022**, *12*, 749.
(46) Kratzer, I.; Wernig, K.; Panzenboeck, U.; Bernhart, E.; Reicher, H.; Wronski, R.; Windisch, M.; Hammer, A.; Malle, E.; Zimmer, A.; Sattler, W. Apolipoprotein A-I coating of protamine-oligonucleotide nanoparticles increases particle uptake and transcytosis in an in vitro model of the blood-brain barrier. *J. Controlled Release* **2007**, *117*, 301−311.

https://doi.org/10.1021/acsomega.2c04440
ACS Omega 2022, 7, 37589−37599

(47) Wang, C.; Chen, B.; He, M.; Hu, B. Composition of intracellular protein corona around nanoparticles during internalization. *ACS Nano* **2021**, *15*, 3108−3122.

https://doi.org/10.1021/acsomega.2c04440
ACS Omega 2022, 7, 37589−37599